

# Ab initio calculations of $H_{c2}$ for Nb, NbSe<sub>2</sub>, and MgB<sub>2</sub>

Masao Arai\*

Computational Materials Science Center, National Institute for Materials Science, Tsukuba, 305-0044, Japan

Takafumi Kita

Division of Physics, Hokkaido University, Sapporo 060-0810, Japan

(Dated: today)

We report on quantitative calculations of the upper critical field  $H_{c2}$  for clean type-II superconductors Nb, NbSe<sub>2</sub>, and MgB<sub>2</sub> using Fermi surfaces from *ab initio* electronic structure calculations. The results for Nb and NbSe<sub>2</sub> excellently reproduce both temperature and directional dependences of measured  $H_{c2}$  curves without any adjustable parameters, including marked upward curvature of NbSe<sub>2</sub> near  $T_c$ . As for MgB<sub>2</sub>, a good fit is obtained for a  $\pi/\sigma$  gap ratio of  $\sim 0.3$ , which is close to the value from a first-principles strong-coupling theory [H. J. Choi *et al.* *Nature*, **418** 758 (2002)]. Our results indicate essential importance of Fermi surface anisotropy for describing  $H_{c2}$ .

PACS numbers: 74.25.Op, 71.18.+y, 74.25.Jb

Quantitative descriptions of nature form an integral part of physics. In this context, the density-functional theory for normal-state electronic structures has substantially enhanced our understanding on materials and also made materials design possible [1]. The purpose of the present paper is to extend those calculations in the normal state to type-II superconductors in magnetic fields to perform systematic calculations of  $H_{c2}$ .

The upper critical field  $H_{c2}$  is one of the most fundamental quantities in type-II superconductors. From the early stage of research on type-II superconductors [2], it has been recognized that Fermi surface anisotropy has significant effects on  $H_{c2}$ . However, most of the calculations performed so far on  $H_{c2}$  have used simplified model Fermi surfaces and/or phenomenological fitting parameters. Due to this lack of *ab initio*-type calculations, our understanding on  $H_{c2}$  remains at a rather primitive level. The only exception is the work by Butler on bcc Nb [3], where he obtained an excellent agreement with experiments [4, 5] by using Fermi surfaces and electron-phonon interactions from his *ab initio* calculations. Extending this calculation to other materials is expected to improve our understanding on  $H_{c2}$  considerably.

Recently we have derived an  $H_{c2}$  equation applicable to low-symmetry crystals, including Fermi surface anisotropy, gap anisotropy, impurity scatterings, and strong electron-phonon interactions [6]. We here concentrate on the role of Fermi surface anisotropy and carry out clean-limit weak-coupling calculations of  $H_{c2}$  for Nb, NbSe<sub>2</sub>, and MgB<sub>2</sub>. Sauerzopf *et al.* [7] performed a careful experiment on  $H_{c2}$  of high-purity Nb to report some discrepancies from preceding experiments [4, 5] and the theory by Butler [3]. Also,  $H_{c2}$  curves of NbSe<sub>2</sub> [8, 9, 10] and MgB<sub>2</sub> [11, 12, 13, 14] remains essentially unexplained quantitatively. We here treat Fermi surface anisotropy without any adjustable parameters by using energy band data from first-principles electronic structure calculations.

We have determined  $H_{c2}$  by requiring that the smallest eigenvalue of the following matrix be zero [6]:

$$\mathcal{A}_{NN'} \equiv \delta_{NN'} \ln \frac{T}{T_c} + 2\pi T \sum_{n=0}^{\infty} \left[ \frac{\delta_{NN'}}{\varepsilon_n} - \langle \phi^2 \mathcal{K}_{NN'} \rangle \right]. \quad (1)$$

Here  $N$  denotes the Landau level in expanding the pair potential and  $\varepsilon_n \equiv (2n+1)\pi T$  is the Matsubara frequency ( $k_B = \hbar = 1$ ). The function  $\phi(\mathbf{k}_F)$  specifies gap anisotropy, which is normalized in such a way that the Fermi-surface average  $\langle \phi^2 \rangle$  is equal to unity. The matrix  $\mathcal{K} = \mathcal{K}(\varepsilon_n, \mathbf{k}_F, H)$  is given explicitly in Ref. 6. We need to evaluate the average  $\langle \phi^2 \mathcal{K} \rangle$  in Eq. (1) appropriately.

We have obtained Fermi surfaces and velocities from electronic structure calculations within the local density approximation (LDA) [1], using the WIEN2k package [15] which is based on the full-potential linear augmented plane wave method. The self-consistent calculations have been performed by using finite  $\mathbf{k}$  points. Then we have fitted the energy bands by linear combinations of the star functions [16, 17, 18] to construct Fermi surfaces on finer mesh points. Integrations over Fermi surfaces have been performed by the linear tetrahedron method [19]. We have checked the convergence by increasing  $\mathbf{k}$  points.

We shall focus on the temperature and directional dependences of  $H_{c2}$  and use the reduced quantities  $t \equiv T/T_c$  and  $h^*(t) \equiv \frac{H_{c2}(t)}{-dH_{c2}(t)/dt|_{t=1}}$ . When it becomes relevant, the absolute value of  $H_{c2}$  is fixed by using an experimental value at a particular temperature and field direction. This procedure is similar in the normal state to incorporating many-body mass enhancement by using a single point of de Haas-van Alphen data. We have fixed  $\phi(\mathbf{k}_F) = 1$  for Nb and NbSe<sub>2</sub>, since gap anisotropy may not be substantial in these materials. The spin-orbit interaction have been included self-consistently for NbSe<sub>2</sub>.

*bcc Nb* — We first consider temperature dependence of  $H_{c2}$  in Nb. Figure 1 shows theoretical curves for the angle averaged critical field  $\bar{h}^*(t)$  in comparison with the

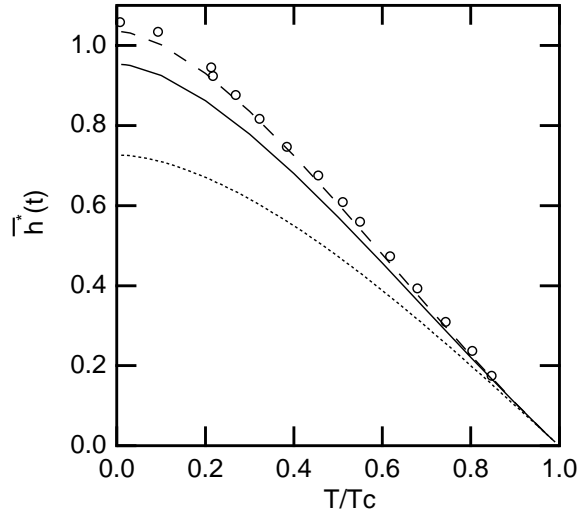


FIG. 1: Normalized angle averaged  $H_{c2}$  for Nb. Open circles are the experiment of Ref. 7. The solid line is obtained by using the Fermi surface from the LDA calculation, whereas the dotted line is the Helfand-Werthamer curve for the spherical Fermi surface. The dashed line incorporates the difference in mass renormalization among different Fermi surface sheets.

experiment by Sauerzopf *et al.* (circles) [7]. The solid line with  $\bar{h}^*(0) = 0.96$  has been obtained as above by using the Fermi surface from the LDA calculation, whereas the dotted line with  $\bar{h}^*(0) = 0.73$  is the Helfand-Werthamer result [20] for the spherical Fermi surface. Considering that there are no adjustable parameters, our result (solid line) shows a fairly good agreement with the experiment, improving on the Helfand-Werthamer curve substantially. However, the value  $\bar{h}^*(0) = 0.96$  still falls well below the experimental value  $\bar{h}^*(0) = 1.06$ .

We attribute this discrepancy to the difference in many-body mass enhancement among different Fermi-surface sheets. According to Butler's calculation [3], strong but  $\mathbf{k}$ -independent electron-phonon interactions cannot cure the discrepancy, since they merely bring an overall enhancement of  $H_{c2}$  but change temperature and directional dependences of  $\bar{h}^*(t)$  by less than 2%. On the other hand, Crabtree *et al.* [21] found from their analysis on de-Haas van Alphen experiments that the electron-phonon renormalization factor  $\lambda_n(\mathbf{k}_F)$  differs substantially by more than 30% among the three Fermi-surface sheets ( $n = 1, 2, 3$ ) of Nb, although it does not vary appreciably within each sheet. Hence we have performed another calculation of  $H_{c2}$  using the scaled Fermi velocity  $\tilde{\mathbf{v}}_n(\mathbf{k}_F) = \mathbf{v}_n(\mathbf{k}_F)/(1 + \lambda_n)$ , where  $\mathbf{v}_n(\mathbf{k}_F)$  is the bare Fermi velocity from the LDA calculation and  $\lambda_n$  is a sheet-dependent scaling factor taken from Ref. 21. This yields the dashed line in Fig. 1 with  $\bar{h}^*(0) = 1.03$ , showing a considerable improvement on the bare result. This fact indicates the importance of band and momentum dependences of the electron-phonon couplings. It is

an interesting problem in the future to see whether the effects are reproduced naturally through a first-principles strong-coupling calculation of  $H_{c2}$ .

We next discuss angular dependence of  $H_{c2}$  in Nb. This dependence for cubic materials has been studied by expanding the relative anisotropy  $H_{c2}/\bar{H}_{c2}$  as [7, 22]

$$H_{c2}(\Omega, t)/\bar{H}_{c2}(t) = 1 + \sum_{l=4,6,8,\dots} a_l(t) P_l(\Omega). \quad (2)$$

Here  $\Omega$  denotes direction of the field and  $P_l$ 's are cubic harmonics [23] invariant under cubic symmetry operations and constructed as linear combinations of the spherical harmonics. The coefficients  $a_l(t)$  specify the  $H_{c2}$  anisotropy at temperature  $t$ . After the work of Butler [3], Sauerzopf *et al.* [7] carried out a very careful and detailed experiment on  $a_l(t)$ . Hence it is very interesting to see whether  $a_l$ 's can also be reproduced by *ab initio* calculations. We have evaluated  $a_l$ 's by least square fittings for  $H_{c2}$  computed over 50 different directions.

Figure 2 compares calculated  $a_l(t)$  ( $l=4, 6, 8, 10$ ) with the experiment by Sauerzopf *et al.* [7]. The agreements are good, especially for the dominant  $a_4(t)$ . For example, the change in the curvature of  $a_4(t)$  around  $t \approx 0.6$  is excellently reproduced. This is not the case for the second-largest contribution  $a_6(t)$ , however, and the calculated curve reproduces only 60% of the experimental value at  $t=0$ . An improvement is observed by introducing the Fermi-surface-dependent renormalization factor  $\lambda_n$  in the calculation (dashed line), but there still remains an appreciable deviation. This discrepancy may be attributed to the small gap anisotropy which may be present in Nb. Indeed, Seidl *et al.* [22] reported that the gap anisotropy has a dominant effect on the  $a_6$  term. However, their analysis may not be reliable quantitatively, especially near  $t=0$ , since they applied a theory by Teichler [24] which incorporate only the lowest-order corrections from the gap and Fermi-surface anisotropies. The discrepancy may be removed completely by a first-principles strong-coupling calculation of  $H_{c2}$  where the gap anisotropy is naturally included.

*NbSe<sub>2</sub>* — The hexagonal transition metal dichalcogenide 2H-NbSe<sub>2</sub> has been studied extensively as a prototype of anisotropic layered superconductors. Nb atoms form triangular lattices in the *ab* plane, which stack along the *c* axis with two Se layers between them. At low temperatures preceding superconductivity, NbSe<sub>2</sub> undergoes an incommensurate charge-density-wave (CDW) transition. Several groups [8, 9, 10] studied  $H_{c2}$  of NbSe<sub>2</sub> and Nb<sub>1-x</sub>Ta<sub>x</sub>Se<sub>2</sub>, where  $H_{c2\parallel}$  for the magnetic field along the *ab* plane was observed by more than 3 times larger than  $H_{c2\perp}$  for the field along the *c* axis at  $T=0$ . Another characteristic feature is the marked positive curvature of  $H_{c2\parallel}$  near  $T_c$ . However, no quantitative calculations using detailed Fermi surfaces have been performed yet.

We have evaluated  $H_{c2}$  using the Fermi surface from the LDA calculation, ignoring any effects of the CDW

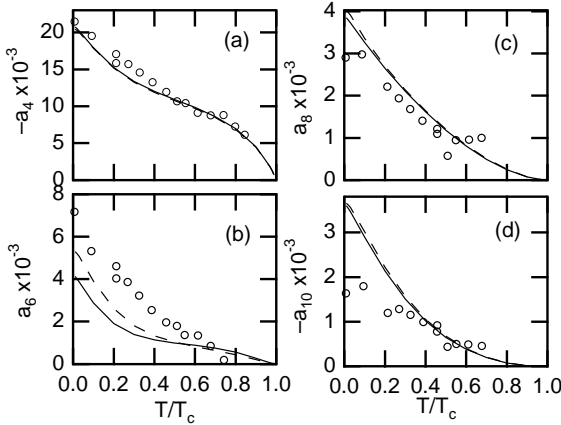


FIG. 2: Anisotropy coefficients  $a_l$  of Nb as a function of temperature for  $l = 4, 6, 8, 10$ . Solid lines are obtained by a bare LDA calculation, whereas dashed lines denote results using the renormalized Fermi velocity  $\tilde{v}_n(\mathbf{k}_F) = v_n(\mathbf{k}_F)/(1 + \lambda_n)$ . Open circles are experiments by Sauerzopf *et al.* [7].

instability. Calculated energy bands and Fermi surface agree well with a previous one [25]. The Fermi surface can be classified into two groups. The first one is cylindrical sheets, and the other is a small hole pocket around  $\Gamma$  point which looks like a flattened spheroid.

Figure 3 shows calculated  $H_{c2\parallel}$  and  $H_{c2\perp}$  curves in comparison with a couple of experiments [8, 10]. Temperature dependence of the anisotropy parameter  $\gamma \equiv H_{c2\parallel}/H_{c2\perp}$  is also shown in the inset. We observe good agreements between the theory and experiments for both field directions. Especially, the positive curvature of  $H_{c2\parallel}$  has been reproduced excellently. Although this positive curvature has been observed commonly in anisotropic superconductors [26], its origin has not been identified clearly so far. Thus, we have shown explicitly that Fermi surface anisotropy adds quite a variety to  $H_{c2}$  curves. The reduced critical field  $h^*(t)$  is also very anisotropic, reaching  $h_{\parallel}^*(0) = 1.73$  and  $h_{\perp}^*(0) = 0.68$  in our calculation. If we ignore the small Fermi surface sheet around  $\Gamma$  point, the agreement becomes worse as shown by the dashed line. Thus, the small Fermi surface sheet cannot be neglected for the quantitative understanding of  $H_{c2}$ .

$MgB_2$  — Superconductivity in  $MgB_2$  found by Nagamatsu *et al.* [27] has attracted much attention. Besides its high transition temperature  $\sim 40K$ , it has a unique feature that the energy gap  $\Delta$  differs substantially in magnitude between  $\sigma$ - and  $\pi$ -bands, as predicted by theories [28, 29] and confirmed by experiments [30, 31, 32]. A first-principles calculation by Choi *et al.* [29] has yielded  $\Delta_{\sigma} \sim 6.8\text{meV}$  and  $\Delta_{\pi} \sim 1.8\text{meV}$  on the average as  $T \rightarrow 0$ .

Experiments on  $H_{c2}$  of uniaxial  $MgB_2$  single crystals have been reported by several groups [11, 12, 13, 14]. Miranović *et al.* [33] performed a calculation of  $H_{c2}$  adopting

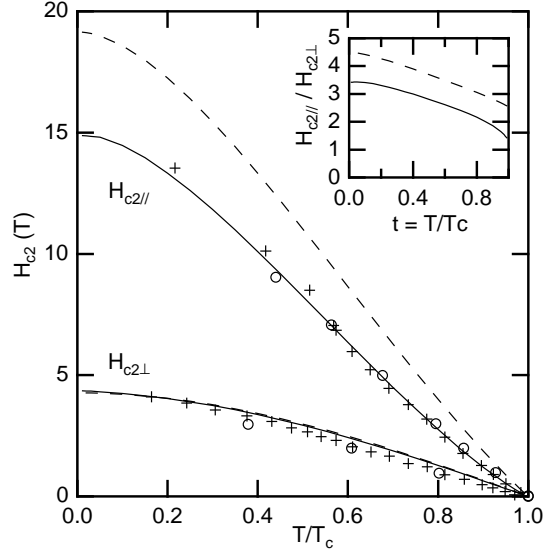


FIG. 3:  $H_{c2\parallel}$  and  $H_{c2\perp}$  of  $NbSe_2$  as a function of temperature. Crosses and open circles are experiments of Ref. 8 and Ref. 10, respectively. The solid lines are from the LDA calculation. If we ignore the Fermi surface around  $\Gamma$  point, the dashed lines result. The inset plots calculated anisotropy ratio  $H_{c2\parallel}/H_{c2\perp}$ .

a model Fermi surface with two spheroids, which yielded a qualitative agreement with observed  $H_{c2}$ . We have carried out a more detailed calculation using the Fermi surface from the LDA calculation. As seen above, detailed Fermi-surface structures are indispensable for the quantitative understanding of  $H_{c2}$ . As for the gap anisotropy, we have incorporated the ratio  $\alpha \equiv \Delta_{\pi}/\Delta_{\sigma}$  at  $T=0$  as a single parameter in the calculation.

Figure 4 plots calculated  $H_{c2\parallel}$  and  $H_{c2\perp}$  for  $MgB_2$  using three different values of  $\alpha$ . When we assume an isotropic gap of  $\alpha = 1$ , we could not describe the experimental anisotropy  $H_{c2\parallel}/H_{c2\perp}$ . The anisotropy of  $0.6 \lesssim t \lesssim 1.0$  has been reproduced most completely for the choice  $\alpha \sim 0.3$ . This value is close to the one obtained by Choi *et al.* [29] and consistent with the model calculation by Miranović *et al.* [33]. Thus, the present calculation provides an additional support for the existence of two energy gaps via a detailed calculation of  $H_{c2}$ . The reduced critical field  $h^*(t)$  is very anisotropic as  $h_{\parallel}^*(0) = 1.64$  and  $h_{\perp}^*(0) = 0.67$  for  $\alpha = 0.3$ . However, calculated  $H_{c2}$  for  $\alpha = 0.3$  shows larger anisotropy at lower temperatures than the experimental one. This discrepancy may be removed completely by incorporating effects neglected here, such as strong electron-phonon interactions, Pauli paramagnetism, etc.

In summary, we have evaluated  $H_{c2}$  of three classic type-II superconductors using Fermi surfaces from first-principles electronic structure calculations. For Nb and  $NbSe_2$  whose superconducting gap anisotropy may not be

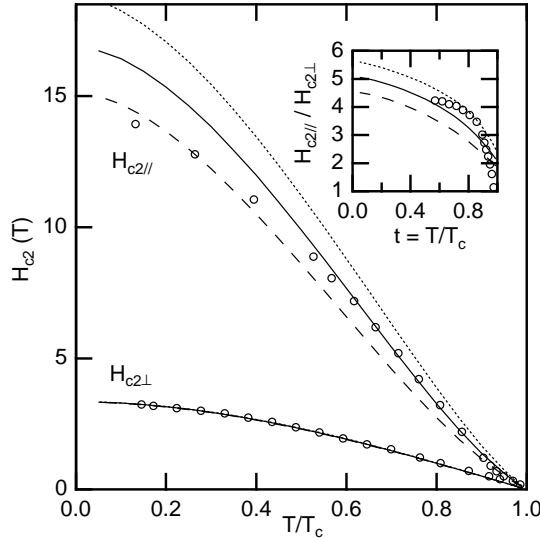


FIG. 4:  $H_{c2}$  of  $\text{MgB}_2$  as a function of temperature. Open circles are experiments of Ref. 12. Calculated  $H_{c2}$  curves for  $\Delta_\pi/\Delta_\sigma = 0.25, 0.3$ , and  $0.35$  are shown by dotted, solid and dashed lines, respectively. The inset shows a comparison of the anisotropy ratio  $H_{c2\parallel}/H_{c2\perp}$ .

significant, calculated  $H_{c2}$  curves satisfactory reproduce experimental temperature and directional dependences of  $H_{c2}$  without any adjustable parameters. As for  $\text{MgB}_2$ , a good agreement with experiments follows if we choose the gap ratio  $\Delta_\pi/\Delta_\sigma \sim 0.3$ . Thus, the present study has clarified unambiguously the necessity of incorporating detailed Fermi surface structures in the calculation of  $H_{c2}$ . Such calculations will also form a basic starting point to discuss other contributions, and we may obtain unique information about superconducting gap anisotropy, etc., by comparing calculated and experimental  $H_{c2}$  curves.

We would like to thank to K. Kobayashi for valuable discussions. This research is supported by a Grant-in-Aid for Scientific Research from Ministry of Education, Culture, Sports, Science, and Technology of Japan.

—

\* Electronic address: arai.masao@nims.go.jp

- [1] R. O. Jones and O. Gunnarsson, Rev. Mod. Phys. **61**, 689 (1989).
- [2] P. C. Hohenberg and N. R. Werthamer, Phys. Rev. **153**, 493 (1967).
- [3] W. H. Butler, Phys. Rev. Lett. **44**, 1516 (1980).
- [4] S. J. Williamson, Phys. Rev. B **2**, 3545 (1970).
- [5] H. Kerchner, D. Christen, and S. Sekula, Phys. Rev. B **21**, 86 (1980).
- [6] T. Kita and M. Arai, cond-mat/040331.
- [7] F. M. Sauerzopf, E. Moser, H. W. Weber, and F. A.

- Schmidt, J. Low. Tem. Phys. **66**, 191 (1987).
- [8] N. Toyota, H. Nakatsuji, K. Noto, A. Hoshi, N. Kobayashi, Y. Muto, and Y. Onodera, J. Low. Temp. Phys. **25**, 485 (1976).
- [9] B. J. Dalrymple and D. E. Prober, J. Low. Temp. Phys. **56**, 545 (1984).
- [10] D. Sanchez, A. Junod, J. Muller, H. Berger, and F. Lévy, Physica B **204**, 167 (1995).
- [11] S. L. Bud'ko, V. G. Kogan, and Canfield, Phys. Rev. B **64**, 180506 (2001).
- [12] M. Zehetmayer, M. Eisterer, J. Jun, S. M. Kazakov, J. Karpinski, A. Wisniewski, and H. W. Weber, Phys. Rev. B **66**, 052505 (2002).
- [13] M. Angst, R. Puzniak, A. Wisniewski, J. Jun, S. M. Kazakov, J. Karpinski, J. Roos, and H. Keller, Phys. Rev. Lett. **88**, 167004 (2002).
- [14] U. Welp, A. Rydh, G. Karapetrov, W. K. Kwok, G. W. Crabtree, C. Marcenat, L. Paulius, T. Klein, J. Marcus, K. H. P. Kim, et al., Phys. Rev. B **67**, 012505 (2003).
- [15] P. Blaha, K. Schwarz, G. K. H. Madsen, D. Kvaniscka, and J. Luitz, WIEN2k, An Augmented Plane Wave + Local Orbitals Program for Calculating Crysal Properties (Karlheinz Schwartz, Techn. Universität Wien, Austria), 2001. ISBN 3-9501031-1-2.
- [16] D. Koelling and J. H. Wood, J. Comput. Phys. **67**, 253 (1986).
- [17] W. E. Pickett, H. Krakauer, and P. B. Allen, Phys. Rev. B **38**, 2721 (1988).
- [18] M. Arai and S. Ikegawa, J. Phys. Soc. Jpn. **72**, 1138 (2003).
- [19] O. Jepsen and O. K. Andersen, Solid State Commun. **9**, 1763 (1971).
- [20] E. Helfand and N. R. Werthamer, Phys. Rev. **147**, 288 (1966).
- [21] G. W. Crabtree, D. H. Dye, D. P. Karim, S. A. Campbell, and J. B. Keterson, Phys. Rev. B **35**, 1728 (1987).
- [22] E. Seidl, H. W. Weber, and H. Teichler, J. Low. Tem. Phys. **30**, 273 (1977).
- [23] F. C. von der Large and H. A. Bethe, Phys. Rev. **71**, 612 (1947).
- [24] H. Teichler, Phys. Stat. Sol. (b) **69**, 501 (1975).
- [25] R. Corcoran, P. Messon, Y. Onuki, P.-A. Probst, M. Springford, K. Takita, H. Harima, G. Y. Guo, and B. L. Gyorffy, J. Phys. Condens. Matter **6**, 4479 (1994).
- [26] J. Woollam, R. Somoano, and P. O'Connor, Phys. Rev. Lett. **32**, 712 (1974).
- [27] J. Nagamatsu, N. Nakagawa, T. Muranaka, Y. Zenitani, and J. Akimitsu, Nature **410**, 63 (2001).
- [28] A. Liu, I. Mazin, , and J. Kortus, Phys. Rev. Lett. **87**, 087005 (2001).
- [29] H. J. Choi, D. Roundy, H. Sun, M. Cohen, and S. G. Louie, Nature **418**, 758 (2002).
- [30] Y. Wang, T. Plackowski, and A. Jumod, Physica C **355**, 179 (2001).
- [31] F. Bouquet, R. F. Fisher, N. E. Philips, D. G. Hinks, and J. D. Jorgensen, Phys. Rev. Lett. **87**, 047001 (2001).
- [32] P. Szabó, P. Samuely, J. Kačmarčík, T. Klein, J. Marcus, D. Fruchart, S. Miraglia, C. Marcenat, and A. Jansen, Phys. Rev. Lett. **87**, 137005 (2001).
- [33] P. Miranović, K. Machida, and V. G. Kogan, J. Phys. Soc. Jpn. **72**, 221 (2003).